Simultaneous Sulfur Dioxide Absorption and Hydrogen Sulfide Generation in an Aqueous Solution of Sodium Sulfide

CHARLES Q. JIA† AND W-K. LU*

Department of Materials Science and Engineering, McMaster University, Hamilton, Ontario L8S 4L7, Canada

In flue gas desulfurization (FGD) processes, elemental sulfur is the desirable end product for SO_2 producers located in remote areas, since it is easier to handle and transport. To convert sulfur dioxide to elemental sulfur via the Claus reaction, hydrogen sulfide is needed as a reductant. In the present work, an attempt was made to generate H_2S from aqueous sodium sulfide using SO_2. The behavior of the $Na_2S_{(aq)}-SO_{2(g)}-H_2S_{(g)}$ system was studied experimentally and by modeling. A three-stage pattern was observed in a semi flow batch reactor (SFBR) in regard to chemical properties of this system. It was concluded that aqueous Na_2S solution can be used to absorb SO_2 in flue gas and to generate H_2S under conditions of the second stage. The simultaneous SO_2 absorption and H_2S generation in an aqueous Na_2S solution were confirmed using a continuous flow tank reactor (CFTR). To simulate both the SFBR and the CFTR, two mathematical models were developed based on chemical equilibria of acid−base reactions and mass and charge balances. Results show that thermodynamic analysis of acid−base reactions can describe the behavior of the $Na_2S_{(aq)}-SO_{2(g)}-H_2S_{(g)}$ system when redox reactions are suppressed.

Introduction

The flue gas desulfurization (FGD) processes are often classified into two groups: "throwaway" and "recycled", depending on the usefulness of the sulfur-containing product generated from the fixed sulfur dioxide. In recycled FGD processes, sulfur dioxide is removed from the flue gas and converted into a useful product. The typical products of recycled FGD processes are sulfuric acid, liquid sulfur dioxide, and elemental sulfur. Sulfuric acid is in general the most economic product in terms of its cost of production. Liquid sulfur dioxide as a byproduct is limited by the size of the market. On the other hand, since elemental sulfur is easier to handle and transport, and is the raw material for many industrial processes, it is a desirable product for sulfur dioxide producers located far away from their customers (*1*).

The existing technologies for elemental sulfur production from sulfur dioxide in flue gas have certain limitations: the high capital cost due to the complexity of the process (*2*), such as the carbonate-based ESI process (*1*), the high cost of operation due to the need of expensive reductants, such as natural gas, or the poor quality of elemental sulfur when coal is used as the reductant.

It is well known that sulfur dioxide reacts with hydrogen sulfide, forming elemental sulfur and water via the Claus reaction:

$$SO_{2(g)} + 2H_2S_{(g)} = \frac{3}{8}S_8 + 2H_2O \qquad (1)$$

To control SO_2 emissions, attempts have been made recently to generate hydrogen sulfide as a reductant. A study on the kinetics of carbonation conversion of aqueous sodium sulfide to hydrogen sulfide showed that hydrogen sulfide generation was limited by the absorption of carbon dioxide (*3*). Since sulfur dioxide is more acidic and more soluble in water than carbon dioxide, the kinetics of hydrogen sulfide generation is expected to be improved by replacing carbon dioxide by sulfur dioxide. In addition to the possible higher efficiency of hydrogen sulfide generation, the flow sheet could be simplified due to the elimination of carbonates on which the ESI process is based (*4*). Accordingly, this investigation has been focused on the behavior of the $Na_2S_{(aq)}-SO_{2(g)}-H_2S_{(g)}$ reacting system to identify conditions for simultaneous SO_2 absorption and H_2S generation.

Chemical Reactions

There are two types of reactions in the $Na_2S_{(aq)}-SO_{2(g)}-H_2S_{(g)}$ system: acid−base reactions and redox reactions. Acid−base reactions generate hydrogen sulfide from sodium sulfide, while redox reactions change the valency of sulfur-containing species.

The absorption of sulfur dioxide and the generation of hydrogen sulfide in an aqueous solution of sodium sulfide may be adequately described using the following chemical reactions. The absorption of sulfur dioxide into an aqueous solution can be described by an interfacial reaction:

$$SO_{2(g)} + H_2O_{(l)} \rightarrow H_2SO_{3(aq)} \qquad (2)$$

Dissociation of sulfurous acid produces bisulfite, sulfite, and H^+ ions according to the following two reactions:

$$H_2SO_{3(aq)} \rightleftarrows HSO_3^-{}_{(aq)} + H^+{}_{(aq)} \qquad (3)$$

$$HSO_3^-{}_{(aq)} \rightleftarrows SO_3^{2-}{}_{(aq)} + H^+{}_{(aq)} \qquad (4)$$

Hydrogen ions supplied by dissociation of sulfurous acid react with soluble sulfide ions (which enter the system as sodium sulfide) to form bisulfide and aqueous hydrogen sulfide. These two reactions are written as follows:

$$S^{2-}{}_{(aq)} + H^+{}_{(aq)} \rightleftarrows HS^-{}_{(aq)} \qquad (5)$$

$$HS^-{}_{(aq)} + H^+{}_{(aq)} \rightleftarrows H_2S_{(aq)} \qquad (6)$$

† Present address: Department of Chemical Engineering and Applied Chemistry, University of Toronto, Toronto, Ontario M5S 1A4, Canada.

0013-936X/96/0930-0377$12.00/0

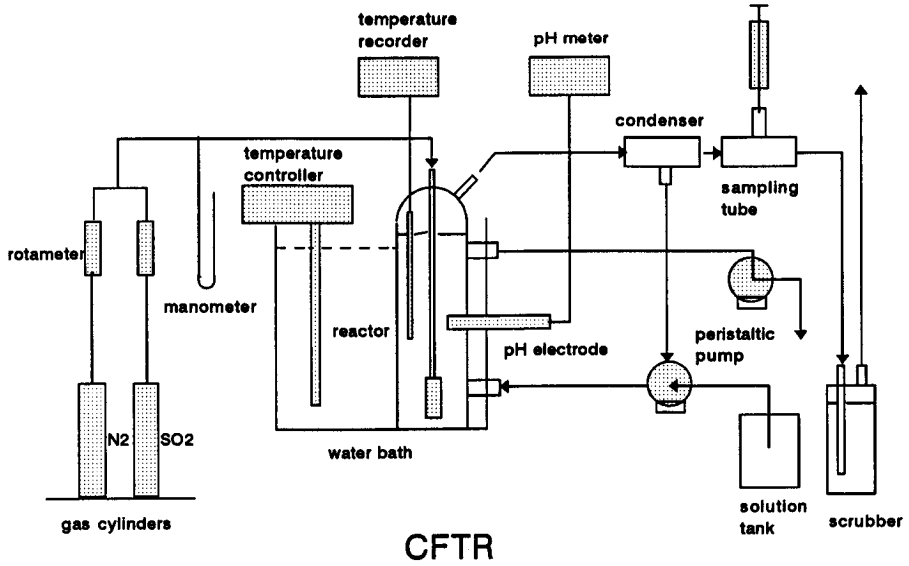

FIGURE 1. Schematic drawing of the experimental set up for the CFTR study (in the SFBR study no pump was used to feed and withdraw liquid to and from the reactor).

Desorption of hydrogen sulfide is a transfer of H_2S from the aqueous to the gaseous phase, which can be represented by the following interfacial reaction:

$$H_2S_{(aq)} \rightarrow H_2S_{(g)} \quad (7)$$

The overall reaction, based on the above six mechanistic equations, may be written in two ways depending on whether bisulfite or sulfite is produced.

$$Na_2S_{(aq)} + 2SO_{2(g)} + 2H_2O_{(1)} \rightarrow H_2S_{(g)} + 2NaHSO_{3(aq)} \quad (8)$$

$$Na_2S_{(aq)} + SO_{2(g)} + H_2O_{(1)} \rightarrow H_2S_{(g)} + Na_2SO_{3(aq)} \quad (9)$$

Without oxygen in the system, sulfur dioxide is the only oxidizer. Sulfur dioxide can oxidize aqueous sulfide (including aqueous H_2S), forming elemental sulfur. For aqueous hydrogen sulfide, it is called wet Claus reaction.

$$2H_2S_{(aq)} + SO_{2(aq)} \rightarrow \frac{3}{8}S_{8(s)} + 2H_2O_{(1)} \quad (10)$$

This reaction is highly exothermic (*5*) and, therefore, thermodynamically less favorable at higher temperatures.

Elemental sulfur produced by redox reactions can be dissolved by reaction with sulfide ions in a basic solution to form polysulfide (S_x^{2-}) according to the following reaction (*6*):

$$S^{2-}{}_{(aq)} + \frac{(x-1)}{8}S_{8(s)} \rightleftharpoons S_x{}^{2-}{}_{(aq)} \quad (11)$$

It was reported that the polysulfuration index, x in S_x^{2-}, is between 2 and 5 in an aqueous solution (*7*, *8*). Elemental sulfur formed may disproportionate in a basic aqueous solution to form bisulfide and thiosulfate (*9*, *10*) via the following reaction:

$$\frac{1}{2}S_8 + 4OH^-{}_{(aq)} \rightleftharpoons S_2O_3{}^{2-}{}_{(aq)} + 2HS^-{}_{(aq)} + H_2O \quad (12)$$

Elemental sulfur may also react with sulfite to form thiosulfate in an alkali sulfite solution (*11*) according to the following reaction:

$$SO_3{}^{2-}{}_{(aq)} + \frac{1}{8}S_8 \rightleftharpoons S_2O_3{}^{2-}{}_{(aq)} \quad (13)$$

In fact, this is the reaction usually used in the commercial production of alkali thiosulfate. Both reactions 12 and 13 are exothermic (*5*) and less favored thermodynamically at higher temperatures.

As a result of redox reactions, a fraction of sulfide is converted into thiosulfate. Since redox reactions consume sulfide, they are undesirable when the intended product is hydrogen sulfide.

Experimental Section

Apparatus. Two types of experiments were conducted by using a semi flow batch reactor (SFBR) and a continuous flow tank reactor (CFTR). Experimental setups for the SFBR and the CFTR studies were essentially similar. In the SFBR study, a gaseous mixture of SO_2-N_2 was continuously fed into a reactor containing aqueous Na_2S solution without adding fresh Na_2S solution during the course of the reaction. In the CFTR study, both the SO_2-N_2 gaseous mixture and the fresh Na_2S solution were continuously fed into the reactor, when the spent solution was removed from the reactor continuously to maintain a constant volume.

As shown in Figure 1, the reactor was immersed in a water bath whose temperature was controlled to within ±1.0 °C by a Brinkmann circulator (Model IC-2). Sulfur dioxide and nitrogen were delivered separately from gas cylinders and then mixed to have a predetermined composition. Two rotameters, calibrated from time to time using the soap bubble method, were used to monitor the flow rates of sulfur dioxide and nitrogen. Between the rotameter and the reactor, there was a U-tube manometer which monitored the back pressure of the reactor. The exist gas from the reactor passed through a condenser to remove water vapor from the exit gas. The condensed water was fed back to the reactor to maintain the amount of water in the system. The exit gas from the condenser was guided into a sampling tube, where gas samples were taken for the gas chromatograph analysis. To prevent the leakage of hydrogen sulfide into the atmosphere, the exit gas from the sampler was fed into aqueous NaOH solution in scrubbers before it was released to the fume hood exhaust. In addition

to the basic setup for both SFBR and CFTR experiments, a two-head peristaltic metering pump (DUNGEY PS series) was utilized in the CFTR experiments to feed Na_2S solution into and withdraw spent solution from the reactor.

The glass reactor (200 mm H × 50 mm i.d.) had three outlets on the side. One of them was used to insert a pH electrode. The other two were designed to feed fresh solution to and withdraw spent solution from the reactor. Two outlets on the top of the reactor were used to feed and withdraw gases and to mount the thermocouple. The gas was introduced through a fritted cylinder to reduce bubble size. The fritted cylinder was 12 mm in diameter and 20 mm long with pore size in the range from 40 to 60 μm.

Reagents and Chemical Analysis. Anhydrous sulfur dioxide (99.98 vol %), the electronic grade hydrogen sulfide (> 99.999 vol %), the U.H.P. grade nitrogen (> 99.999 vol %), and the standard gas mixtures for the calibration of the gas chromatograph (GC) were supplied by Canadian Liquid Air Ltd. Reagent grade $Na_2S{\cdot}9H_2O$ crystals supplied by Fisher Scientific were used to prepare aqueous Na_2S solution. Solutions were prepared by dissolving $Na_2S{\cdot}9H_2O$ in distilled water. The actual concentration of sulfide ion in solution was determined by iodometric titration (*11*). A six-sample standard deviation and relative standard deviation for a solution of 1.67 M were determined to be 0.035 M and 2.2%.

A GC (SHIMADZU GC-9A) with a thermal conductivity detector (TCD) was used to analyze gas compositions. The column used was HayeSep Q (8 ft × 1/8 in., 80/100 mesh) supplied by SUPELCO Separation Technologies and was capable of separating N_2, SO_2, and H_2S with helium as a carry gas. The oven temperature was controlled at 100 °C within ±0.1 °C. The precision of measurements was determined by using the standard gaseous mixture. For 10 measurements of SO_2-N_2 mixture with 10% SO_2, the sample standard deviation was determined to be 0.036%. For gas mixtures with 5% and 10% H_2S, the 10-sample standard deviations were 0.028% and 0.027%, respectively.

The pH value of the solution was monitored continuously. A pH meter (Omega RD-2010) equipped with sensitivity and temperature compensation controls was used. The relative accuracy was ±0.1% of full scale ($0 \leq pH \leq 14$) on the chart recorder made by Omega Engineering Co. The readability was 0.05 pH unit for the meter with standard scale. The combined glass electrode was gel-filled with two junctions.

Mathematical Models

Two mathematical models were developed to simulate reactions in both the SFBR and CFTR. These models were based on chemical equilibria of acid−base reactions and mass and charge balances in a well mixed system.

Semi Flow Batch Reactor (SFBR) Model. Six assumptions are made to define this model: (1) no redox reaction occurs in the system; (2) both liquid and gaseous phases are well mixed; (3) chemical reactions in the liquid phase are so fast that all aqueous species in the liquid phase are in thermodynamic equilibrium (thermal and chemical); (4) absorption of SO_2 by the liquid phase is faster than supply of SO_2 by the feed gas; (5) the exit gas is in thermodynamic equilibrium with the liquid phase; and (6) both the gaseous and the aqueous phases are ideal.

Clearly, assumption 1 is acceptable only when the rate of redox reactions is much lower than that of acid−base reactions, i.e., when the fraction of sodium sulfide converted to hydrogen sulfide is close to 1. As will be shown later, this fraction can be over 0.9 at 90 °C. Assumption 2 is based on a series of experiments in which the effect of gas flow rate on hydrogen sulfide generation was studied (*5*). These experiments showed that H_2S generation was not limited by mixing under the conditions studied. Assumption 3 is valid only when reactions 3−6 and the reaction between OH^- and H^+ are very fast in a well-mixed system, which is likely true for proton transfer reactions in an aqueous medium. Assumption 4 is supported by studies on the kinetics of reaction 2 by several authors (*12*, *13*) and by the complete absorption of SO_2 as shown in this study. The validity of assumption 5 depends on the rate of desorption of H_2S (reaction 7). A study on the effect of bubble size (*5*) showed that the change in liquid/gas interfacial area did not result in any noticeable change in H_2S content in exit gas, which supports the assumption. When total pressure is low, the gas is usually ideal. For an aqueous solution with very high ionic strength, ideal solution is recommended (*14*).

TABLE 1
Summary of Variables in the SFBR Model[a]

variables	description	units
$[Na^+]$	sodium ion content	mol/L (M)
$[H^+]$	hydrogen ion content	mol/L (M)
$[OH^-]$	hydroxide ion content	mol/L (M)
$[S^{2-}]$	sulphide ion content	mol/L (M)
$[HS^-]$	bisulphide ion content	mol/L (M)
$[H_2S_{aq}]$	aqueous H_2S content	mol/L (M)
$[SO_3^{2-}]$	sulphite ion content	mol/L (M)
$[HSO_3^-]$	bisulphite ion content	mol/L (M)
$[H_2SO_3]$	sulphurous acid content	mol/L (M)
VOL	volume of liquid	L
FLG^i,	flow rate of incoming gas	mol/min
FLG^o	flow rate of outgoing gas	mol/min
$Y^i_{SO_2}$	molar fraction of SO_2	dimensionless
$Y^o_{H_2S}$	molar fraction of H_2S	dimensionless
T	reaction temperature	K

[a] Superscripts i and o stand for the incoming and outgoing streams, respectively.

As shown in Table 1, there are 15 variables in the system, among which volume of liquid and concentration of sodium, flow rate, and SO_2 content of the feed gas and reaction temperature are known. Hence, the number of unknowns is 10. Constraints on the system include equilibrium relations of six chemical reactions, the conservation of three groups of chemical species (S^{4+}-containing species, S^{2-}-containing species, and nitrogen) and charge balance in the solution. Since it was assumed that no redox reaction occurs in this system, valence states of all species remain unchanged. Consequently, there are 10 constraints for 10 unknowns, resulting a mathematically solvable problem. It should be pointed out that the model was built on a dry gas basis, since in the present experiments $Y^o_{H_2S}$ was measured after the removal of water vapor.

Chemical reactions included are reactions 3−7 and the reaction between OH^- and H^+. Standard free energy changes ($\Delta G°$) of the reactions were calculated based on data given by Barner and Scheuermann (*15*), which were determined using the entropy correspondence principle developed by Criss and Cobble (*16*, *17*). The standard reference state for each element is chosen to be the state that is thermodynamically stable at the given temperature and 1 atm pressure. For a gas, the standard state is defined by a hypothetical ideal gas at the given temperature and

a fugacity of 1 atm. The standard state for a solute in aqueous solution is defined by a hypothetical ideal solution at a molality of 1.0. Equilibrium constants of chemical reactions were calculated using the following equation:

$$K = e^{-\Delta G^\circ/RT} \quad (14)$$

The sulfur with a valency of +4 enters the system as sulfur dioxide in the feed gas and remains in the system as sulfite, bisulfite, and sulfurous acid. The mass balance at time t after the commencement of the reaction is described as follows

$$\int_0^t Y^i_{SO_2} FLG^i dt = ([SO_3^{2-}] + [HSO_3^-] + [H_2SO_3])VOL \quad (15)$$

where the left and right hand sides are the total amount of this type of sulfur in the feed gas and in the solution, respectively.

The sulfur with a valency of −2 in this system is originally from sodium sulfide and leaves the system as hydrogen sulfide. The mass balance is described as follows

$$([S^{2-}]^i + [HS^-]^i + [H_2S_{aq}]^i)VOL = \int_0^t Y_{H_2S} FLG^o dt + ([S^{2-}] + [HS^-] + [H_2S_{aq}])VOL \quad (16)$$

where the left and right hand sides are the amount of sulfide added initially to the reactor as Na_2S and the total amount of sulfide leaving the solution as H_2S up to the time t and sulfide which is still in the solution, respectively.

Ions with positive charges are sodium and hydrogen ions, while ions with negative charges are sulfide, bisulfide, sulfite, bisulfite, and hydroxide ions. The charge balance must be maintained according to the following equations:

$$[Na^+] + [H^+] = 2[S^{2-}] + [HS^-] + 2[SO_3^{2-}] + [HSO_3^-] + [OH^-] \quad (17)$$

where the left and right hand sides are the molar concentrations of positive- and negative-charged ions in the solution, respectively.

Continuous Flow Tank Reactor (CFTR) Model. Assumptions made in the CFTR model are the same as that in the SFBR model. Among the variables, properties of incoming streams are $[Na^+]^i$, $[H^+]^i$, $[OH^-]^i$, $[S^{2-}]^i$, $[HS^-]^i$, $[H_2S_{aq}]^i$, $[SO_3^{2-}]^i$, $[HSO_3^-]^i$, $[H_2SO_3]^i$, FLL^i, $Y^i_{SO_2}$, FLG^i, and T, which are known. Properties of outgoing streams are $[H^+]^o$, $[OH^-]^o$, $[S^{2-}]^o$, $[HS^-]^o$, $[H_2S_{aq}]^o$, $[SO_3^{2-}]^o$, $[HSO_3^-]^o$, $[H_2SO_3]^o$, FLL^o, FLG^o, and $Y^o_{H_2S}$, which are unknown and depend on the properties of in-coming streams. Among them, FLL and FLG are flow rates of liquid and gaseous streams. Y_A is the molar fraction of substance A. Superscripts "i" and "o" stand for incoming (feed) and outgoing (exit) streams, respectively. To solve the 11 unknowns, the 11 constraints are equilibrium constants of six chemical reactions, conservation equations of four groups of chemical species (S^{4+}-containing species, S^{2-}-containing species, hydrogen-containing species, and nitrogen) and charge balance in the solution.

Since most of the relations in the CFTR model are similar to that in the SFBR model, only the conservation of S^{4+}-containing and S^{2-}-containing species are given here. The mass balance of the sulfur with a valency of +4 is written as follows

$$Y^i_{SO_2} FLG^i = ([SO_3^{2-}]^o + [HSO_3^-]^o + [H_2SO_3]^o)FLL^o \quad (18)$$

where $Y^i_{SO_2}$ and FLG^i are the molar fraction of SO_2 and flow rate (mol/min) of incoming gas and FLL^o is the flow rate (L/min) of outgoing liquid.

The sulfur with a valency of −2 enters the system as sodium sulfide in feed solution and leaves the system as hydrogen sulfide according to the following equation

$$([S^{2-}]^i + [HS^-]^i + [H_2S_{aq}]^i)FLL^i = ([S^{2-}]^o + [HS^-]^o + [H_2S_{aq}]^o)FLL^o + Y^o_{H_2S} FLG^o \quad (19)$$

where the left and right hand sides are molar fluxes of S^{2-}-containing species in the incoming and outgoing streams, respectively.

Computational Method. Both the SFBR and CFTR models are nonlinear. The SFBR model consists of a set of 10 nonlinear equations including two integral equations. To solve the equations, MATLAB was used. MATLAB is software which includes a function call named "fsolve". The "fsolve", which is based on the Newtonian iteration method, is designed to solve the nonlinear equation set. Due to the nonlinearity, the solution was sensitive to the initial point selected. For the SFBR model, the equilibrium composition of an aqueous Na_2S solution, which was calculated based on the dissociation constants of Na_2S in water, was used to estimate the initial point. For the CFTR model, the initial point was estimated based on the compositions of the aqueous and gaseous phase determined under the similar conditions using the SFBR model. In addition to the initial point, a small step length was found essential to obtain meaningful results. To ease the convergence, the scaling factors were included in both models, so that the variables had a similar order of magnitude.

Behavior of the $Na_2S_{(aq)}-SO_{2(g)}-H_2S_{(g)}$ System in SFBR

Three-Stage Pattern. When the SO_2-N_2 gaseous mixture was fed continuously into the solution, a three-stage pattern was observed in terms of changes in pH value and gas composition as a function of reaction time which is proportional to the amount of SO_2 fed. As shown in Figure 2, there were two sharp drops in pH value, which corresponded to the beginning of the second and third reaction stages, respectively. Within each of these three stages, decreases in the pH value were relatively small. In addition to the change in pH value, the composition of the exit gas also changed according to this pattern. In the first stage the contents of both sulfur dioxide and hydrogen sulfide in the exit gas were below the detecting limit (10 ppm). The second stage started with the beginning of hydrogen sulfide generation. In the second stage, hydrogen sulfide formed steadily with the complete removal of sulfur dioxide from the feed gas. The third stage began when the generation of hydrogen sulfide stopped. At the beginning of the third stage, sulfur dioxide was detected in the exit gas. Its concentration increased gradually with time.

Figure 3 is a comparison between the computed and measured P_{H_2S} and pH values under conditions of the first and second stage. The agreement is reasonably good, indicating a strong dependence of system behavior on acid−base reactions. The drops of pH at the end of first and

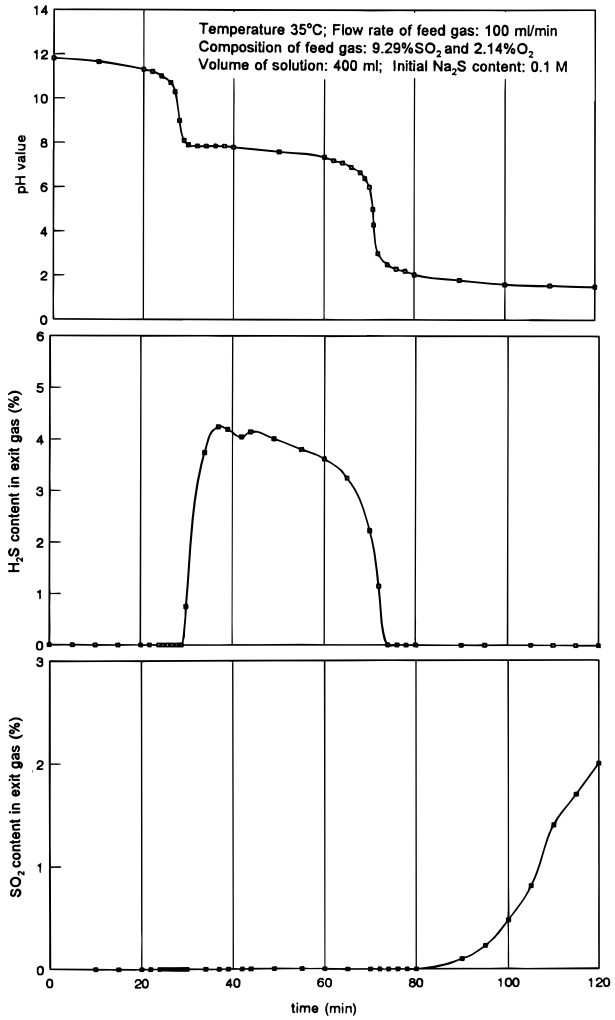

FIGURE 2. Observed three-stage pattern.

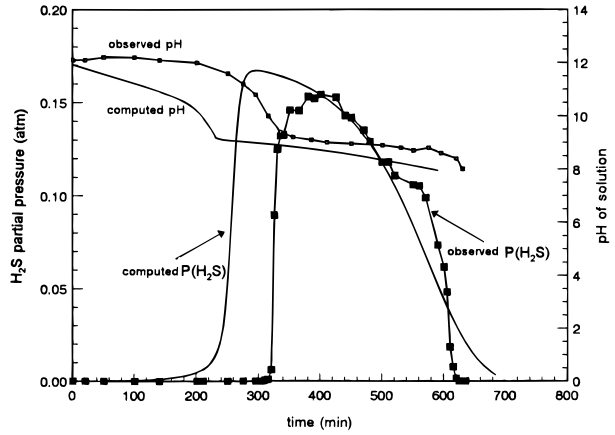

FIGURE 3. Comparison between computed and observed H_2S partial pressures and pH values obtained in SFBR.

second stages likely represent the end of buffering effect produced by reactions 5 and 6. However, in the first stage, the observed pH was higher than the computed one. In addition, the model predicted an earlier release of hydrogen sulfide. These differences are likely due to the fact that in the model redox reactions were excluded. When redox reactions (e.g., the wet Claus reaction) occur, less sulfur dioxide will react with water to produce protons, which may lead to a higher pH. In addition, less sulfide will be available for hydrogen sulfide formation.

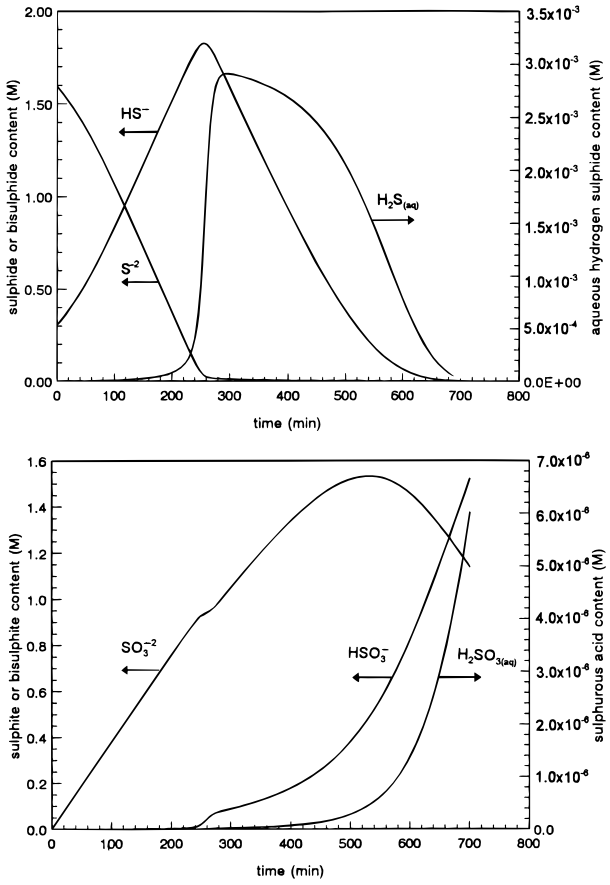

FIGURE 4. Computed changes of solution composition with time in first and second stages (T = 90 °C; VOL = 400 mL; P_{SO_2} = 0.1 atm; FGL = 340 mL/min).

To provide an overall picture, the predicted changes in composition of solution in the first and second stages are presented in Figure 4. Initially, the concentration of sulfide is approximately five times higher than that of bisulfide. In the first stage, the absorption of SO_2 results in a decrease in sulfide concentration and an increase in bisulfide concentration. In the second stage, bisulfide concentration decreases with the release of H_2S as the absorption of SO_2 continues. At the end of the second stage, all sodium sulfide is converted into hydrogen sulfide and no sulfide or bisulfide ions remain in the solution. On the other hand, S^{4+}-containing ions exist as sulfite, bisulfite, and sulfurous acid with their relative amounts determined by thermodynamic relations. The total amount of S^{4+}-containing ions accumulates in the first and second stages as the absorption of sulfur dioxide continues.

Factors Affecting Na_2S Conversion to H_2S. In order to quantify the conversion of sodium sulfide to hydrogen sulfide, a conversion ratio (R) is defined as follows

$$R = \frac{M_{H_2S}}{M_{Na_2S}} \tag{20}$$

where M_{H_2S} and M_{Na_2S} are the total amounts of H_2S generated and Na_2S added in the system initially. It should be pointed out that there is a difference between the R for the SFBR and the R for the CFTR. In the SFBR, the R can reach unity if the redox reactions do not occur. However, in the CFTR the R is always less than unity since the spent solution contains soluble sulfide.

TABLE 2

Comparison between Observed and Computed Partial Pressure of H_2S at 90 °C

condns of feeding streams	measured P_{H_2S} (atm)[a]	computed P_{H_2S} (atm)	difference (%)
no. O_2, no impurity, 7.0% SO_2	0.043 ($n = 17$, $\sigma = 0.0007$)	0.045	4.4
no. O_2, no impurity, 9.8% SO_2	0.058 ($n = 14$, $\sigma = 0.0005$)	0.062	6.4
1.9% O_2, no impurity, 9.5% SO_2	0.055 ($n = 9$, $\sigma = 0.0006$)	0.060	8
1.9% O_2, with impurities, 9.5% SO_2	0.053 ($n = 6$, $\sigma = 0.0008$)	0.060	12

[a] n and σ are the size and the standard deviation of the sample set, respectively.

TABLE 3

Comparison between Observed and Computed Molar Flux Ratios at 90 °C[a]

condns of feeding streams	$F(H_2S)/F(Na_2S)$ obsd	$F(H_2S)/F(Na_2S)$ computed	difference
no O_2, no impurity, 7.0% SO_2	0.96	0.99	3
no O_2, no impurity, 9.8% SO_2	0.94	0.99	5
1.9% O_2, no impurity, 9.5% SO_2	0.87	0.99	12
1.9% O_2, with impurities, 9.5% SO_2	0.86	0.99	14

[a] $F(H_2S)$ and $F(Na_2S)$ are the molar flows of H_2S in dry exit gas and Na_2S in feed solution, respectively.

It was found that both the H_2S strength in the exist gas and the R increased as temperature increased. To investigate the temperature effect, the 8.91% SO_2 feed gas was fed at a rate of 190 mL/min into 400 mL of 0.017 M Na_2S solution at three different temperatures. The R values were determined to be 0.35, 0.41, and 0.52 at 40, 59, and 79 °C, respectively. It is believed that the increased conversion ratio is due to the suppression of the wet Claus reaction at higher temperatures. As mentioned before, the wet Claus reaction is strongly exothermic.

It was observed that the R decreased with the increase of SO_2 strength in the feed gas. When gases containing 10, 21, and 54 vol % SO_2 were fed into 400 mL of 0.017 M Na_2S solution at 79 °C, the R's were 0.52, 0.35, and 0.12, respectively. In spite of the large increase in the sulfur dioxide content, no SO_2 was not detected in the exit gas in the first and second stages, indicating that the SO_2 absorption was fast. The absorbed SO_2 is the reactant in the wet Claus reaction. The decrease in R is likely due to the accelerated wet Claus reaction. The SFBR model predicted a higher peak P_{H_2S} in the exit gas with a higher SO_2 content in the feed gas (*5*). It was observed that the P_{H_2S} changed from about 0.05 to 0.07 atm when the 10% SO_2 feed gas was replaced by 21% SO_2 feed gas. However, the peak value of P_{H_2S} was only about 0.06 atm with the 51% SO_2 feed gas. It is clear that the model is not applicable when the SO_2 strength is high.

When the initial sodium sulfide concentration was increased from 0.017 to 0.166 M, the peak value of P_{H_2S} changed from 0.06 to 0.08 atm. The pH values of the solution in the first and third stages were higher for the more concentrated solution, although the pH value in the second stage fell into the same range regardless the initial concentration of Na_2S. Indeed, the SFBR model predicted a higher peak value of P_{H23} and a higher pH value in the first stage for a more concentrated solution (*5*). It was observed that the R increased slightly from 0.52 to 0.56 when the 0.017 M solution was replaced by the 0.166 M one. It is not clear why a higher Na_2S content resulted in a larger R. One possible reason is that the higher pH may have slowed down the consumption of sulfide by the redox reactions. A higher pH may suppress or enhance the oxidation of aqueous sulfide by oxygen depending on the range of pH. It was reported that an increased pH led to a slower oxidation when the pH was over 11 (*18*). Furthermore, the pH effect varied with the sulfide concentration. It is reasonable to expect an even more complex pattern when the oxidant is sulfur dioxide.

Experimental results have shown that the ratio of Na_2S conversion to H_2S could be enhanced by increasing reaction temperature and the initial sodium sulfide concentration in solution and by decreasing SO_2 concentration in feed gas. For confirmation, 10% SO_2 gas was introduced into 400 mL of 1.9 M Na_2S solution at 90 °C at a rate of 340 mL/min. In the second stage, the concentration of H_2S in exit gas reached 15 vol %, as shown in Figure 3. The R was determined to be 0.81.

Behavior of the $Na_2S_{(aq)}-SO_{2(g)}-H_2S_{(g)}$ System in CFTR

Four experiments were conducted in the CFTR with the variations of SO_2 and O_2 concentration in feed gas and impurity in solution at 90 °C. Results are given in Tables 2 and 3 in the forms of H_2S partial pressure and Na_2S to H_2S conversion ratio. A typical CFTR experiment began with feeding the SO_2-containing gas to 300 mL of 1.44 M Na_2S solution. The system was allowed to pass the first and part of the second stage. After the system was in the state of the later period of the second stage, a predetermined flow of fresh Na_2S solution was turned on to achieve a steady state. The steady state was marked by a constant composition of exit gas and a constant pH value of the solution. It was observed that hydrogen sulfide content in the exit gas depended on the feed ratio of sulfur dioxide to sodium sulfide. There was an optimal SO_2/Na_2S feed ratio at which the content of hydrogen sulfide in exit gas reached a maximum level.

As shown in Table 3, the presence of 1.9% O_2 in the feed gas lowered the conversion ratio from 0.94 to 0.87, indicating oxygen participated in the oxidation of sulfide under conditions studied. It was reported that oxidation of aqueous sulfide has an intermediate O_2SH^- and a final product, elemental sulfur (*6*). The effect of impurities (Fe, Ni, Cu, and Co) on Na_2S conversion to H_2S appeared to be not significant, although it was reported that oxidation of sulfide by O_2 was strongly catalyzed by Ni, Co, Cu, and Fe (*19*). In this study, impurities were introduced to the reactor

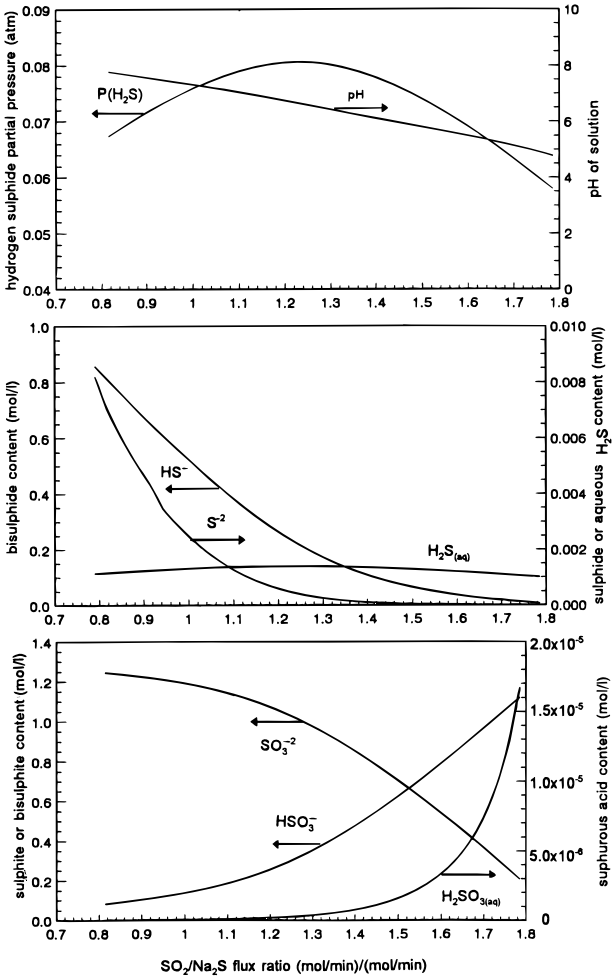

FIGURE 5. Dependence of compositions of outgoing streams on SO_2/Na_2S flux ratio in incoming streams ($T = 90$ °C; $FLG^i = 2.678 \times 10^{-2}$ mol/min; $FLL^i = 2.0 \times 10^{-3}$ L/min; $Y^i_{SO_2} = 0.1$; $[Na_2S]^i$: from 0.75 mol/L to 1.75 mol/L).

in the form of sulfates. The amounts of Fe, Ni, Cu, and Co added were determined by assuming that all impurities would dissolve and form a solution of 300 ppm of Fe, 100 ppm of Ni, 5 ppm of Cu, and 4 ppm of Co. In fact, since solubilities of FeS, NiS, CuS, and CoS in water are 1.24, 0.72, 0.55, and 0.67 ppm at 18 °C (*20*), fractions of dissolved impurities were likely very small due to the high concentration of soluble sulfide in the solution.

The comparison between the observed and computed results is given also in Tables 2 and 3. The observed values and computed values, in view of experimental errors and assumptions made in the computation, agree reasonably well. Again, the difference is thought to be due to the assumption of no redox reaction in the model.

In addition to the simulation of the four experiments, computations were carried out using the CFTR model to study the effect of SO_2/Na_2S molar flux ratio in feed streams. The ratio can be varied by changing the strengths and/or flow rates of feed streams. As an illustration, the initial sodium sulfide concentration in feed liquid was decreased from 1.75 to 0.75 M at a constant temperature (90 °C), while the flow rate of feed gas ($P_{SO_2} = 0.1$ atm) and feed solution were fixed at 2.678×10^{-2} mol/min and 2.0×10^{-3} L/min, respectively. The dependency of P_{H_2S} on exit gas, pH value, and composition of exit solution on the SO_2/Na_2S molar flux is given in Figure 5. Computed results confirm that there is an optimum molar flux ratio at which the equilibrium P_{H_2S} reaches its maximum.

As shown in Figure 5, the contents of both sulfide and bisulfide in exit solution decrease as the sodium sulfide content in feed solution decreases (SO_2/Na_2S ratio increases). The concentration of bisulfide in the exit liquid is approximately 100 times greater than the sulfide concentration. However, the concentrations of sulfite and bisulfite in the exit liquid are of approximately the same order of magnitude. As the sodium sulfide content decreases, the content of sulfite decreases and the content of bisulfite increases in the spent solution. The concentration ratio of sulfite to bisulfite determines the number of moles of SO_2 required to produce 1 mol of H_2S. The concentration of sulfurous acid is orders of magnitude lower than sulfite and bisulfite.

From a practical point of view, a higher H_2S partial pressure and a higher Na_2S to H_2S conversion ratio are both desirable. In CFTR, the Na_2S to H_2S conversion ratio is the ratio of molar flux of hydrogen sulfide in the exit gas to the molar flux of soluble sulfide in feed solution. Clearly, this ratio is dependent on the content of soluble sulfide in the exit solution. In order to achieve a high conversion ratio, the sulfide content in the exit solution should be as low as possible. However, the partial pressure of H_2S in exit gas also depends on the concentration of soluble sulfide/bisulfide in the solution. When H_2S partial pressure is at its maximum the sulfide content in the solution is relatively high (Figure 5). A higher sulfide content in the exit solution represents a lower conversion ratio. Therefore, in some cases a higher H_2S partial pressure in the exit gas may be achieved only at the expense of the conversion ratio or vice versa.

The picture that is emerging is that after sulfur dioxide is absorbed in the aqueous solution it reacts with basic and reductive aqueous sodium sulfide via both acid−base reactions and redox reactions. Acid−base reactions lead to the generation of hydrogen sulfide, while redox reactions produce elemental sulfur and then thiosulfate. Both chemical reactions consume sulfur dioxide or its hydrolysate and, therefore, enhance the absorption of sulfur dioxide. On the other hand, acid−base and redox reactions compete for sodium sulfide. The fraction of sodium sulfide which is converted into hydrogen sulfide can be increased by suppressing redox reactions. To do so, increasing the temperature seems most effective.

Conclusions

For the purpose of converting SO_2 to elemental sulfur via the Claus reaction in which H_2S is required as a reductant, aqueous sodium sulfide is used to generate hydrogen sulfide by reaction with sulfur dioxide. The behavior of the $Na_2S_{(aq)}-SO_{2(g)}-H_2S_{(g)}$ system was studied experimentally and by modeling. On the basis of experimental and computed results, following conclusions are reached.

(1) The $Na_2S_{(aq)}-SO_{2(g)}-H_2S_{(g)}$ reacting system exhibits a three-stage pattern in a semi flow batch reactor (SFBR), which is characterized by the change in the pH of solution with the amount of SO_2 absorbed by the aqueous solution of Na_2S. This behavior can be described using the model based on thermodynamic relations of acid−base reactions.

(2) The simultaneous SO_2 absorbtion and H_2S generation were achieved experimentally under conditions of the second stage in the SFBR and were confirmed under steady state conditions in the continuous flow tank reactor (CFTR).

It was found that the partial pressure of H_2S in the exit gas from the CFTR can be maximized by adjusting the flux ratio of reactants (F_{SO_2}/F_{Na_2S}), which agrees with the computed results.

(3) Incomplete conversions of sodium sulfide to hydrogen sulfide were observed in both SFBR and CFTR. The fraction of sodium sulfide which is converted to hydrogen sulfide can be increased most effectively by increasing temperature, likely due to the suppression of exothermic redox reactions.

(4) In addition to a higher temperature, a higher Na_2S concentration, and a lower SO_2 content in feed gas resulted in a higher conversion ratio of Na_2S to H_2S in SFBR. In the CFTR, the ratio could be over 0.9. The 1.9 vol % oxygen in feed gas lowered the ratio by a few percent, although the effect of impurities (Fe, Ni, Cu, and Co) was not significant.

Acknowledgments

We wish to acknowledge the financial support received from INCO Ltd. and a scholarship to C.Q.J. from the Ontario Government and are grateful to Profs. M. H. I. Baird and E. Hileman at McMaster University and Dr. R. Orr, Dr. B. R. Conard, and Dr. E. Krause at INCO Ltd. for their encouragement and valuable advice.

Literature Cited

(1) Orr, R.; Burnett, T. C. *Proposal for Pilot Plant Demonstration of Sulfur Dioxide Abatement Technology*, 1990, A report submitted to Western Economic Diversification of Canada, INCO Ltd., Manitoba Division, Thompson, Manitoba, Canada.
(2) Strong, H. W.; Heights, S.; Radway, J. E.; Cook, H. A. U.S. Patent No. 3,784,680, patented Jan 8, 1974.
(3) Ng, S. H.; Jia, C. Q.; Lu, W.-K. *Environ. Sci. Technol.* **1993**, *27*, 2158−2161.
(4) Lu, W.-K. A *Research Proposal*, Submitted to Canada Centre for Mineral and Energy Technology, Energy, Mine and Resources Canada, 1989, Department of Materials Science and Engineering, McMaster University, Hamilton, Ontario, Canada.
(5) Jia, C. Q. Ph.D. Thesis, McMaster University, Hamilton, Ontario, Canada, 1993.
(6) Brasted, R. C. *Comprehensive Inorganic Chemistry*; van Nostrand: Princeton, NJ, 1961; Vol. VIII.
(7) Scharzenbach, G.; Fisher, A. *Helv. Chem. Acta.* **1960**, *196*, 1365.
(8) Paschanski, D.; Valensi, *G. J. Chim. Phys.* **1949**, *49*, 602−619.
(9) Tartar, H. V.; Draves, C. Z. *J. Am. Chem. Soc.* **1952**, *46*, 574.
(10) Farr, H. V.; Ruhoff, J. R. U.S. Patent 2,586,459, patented Feb 19, 1952; *Chem. Abstr.* **1952**, *46*, 5276i.
(11) Karchmer, J. H. *The Analytical Chemistry of Sulfur and Its Compounds*; Wiley Interscience: New York, 1970; Part I.
(12) Chang, C. S.; Rochelle, G. T. *Ind. Eng. Chem. Fundam.* **1985**, *24*, 7−11.
(13) Hunger, H.; Lapicque, F.; Storck, A. *J. Chem. Eng. Data* **1990**, *35*, 453−463.
(14) Butler, J. N. *Ionic Equilibrium: A Mathematical Approach*; Addison-Wesley Pub. Co.: Reading, MA, 1964; p 428.
(15) Barner, H. E.; Scheuerman, R. V. *Handbook of Thermochemical Data for Compounds and Aqueous Species*; John Wiley and Sons: New York, 1978.
(16) Criss, C. M.; Cobble, J. W. *J. Am. Chem. Soc.* **1964**, *86*, 5385.
(17) Criss, C. M.; Cobble, J. W. *J. Am. Chem. Soc.* **1964**, *86*, 5390.
(18) Chen, K. Y.; Morris, J. C. *Environ. Sci. Technol.* **1972**, *6*, 529−537.
(19) Chen, K. Y. Ph.D. Thesis, Harvard University, Cambridge, Massachusetts, 1970, pp xiv−xv.
(20) Freier, R. K. *Aqueous Solution: data for inorganic and organic compounds*; W. de Gruyter: Berlin, New York, 1966.

Received for review November 10, 1994. Revised manuscript received September 14, 1995. Accepted September 22, 1995.[⊗]

ES940691X

[⊗] Abstract published in *Advance ACS Abstracts*, December 1, 1995.